

# Printed double-dipole antenna with high directivity using a new feeding structure

Jiangniu Wu<sup>1</sup>, Zhiqin Zhao<sup>1</sup>, Mubarak Sani Ellis<sup>1</sup>, Zaiping Nie<sup>1</sup>, Qing-Huo Liu<sup>2</sup>

<sup>1</sup>School of Electronic Engineering, University of Electronic Science and Technology of China (UESTC), Chengdu, People's Republic of China

<sup>2</sup>Department of Electrical and Computer Engineering, Duke University, Durham, NC 27708, USA

E-mail: zqzhao@uestc.edu.cn

**Abstract:** In this study, a planar printed double-dipole antenna with broadband performance and high directivity is presented. The proposed antenna consists of two dipole elements, two pairs of parallel striplines and a microstrip balun. The main features of the designed antenna are the two dipole elements designed with different lengths and excited in the left and right parts with a pair of antiphase signals. The two dipole elements are designed with different lengths for achieving broadband performance. High directivity is obtained by feeding the two dipole elements with the two antiphase signals. In order to illustrate the effectiveness of the proposed design, a prototype of the proposed antenna is fabricated and measured. Experimental results of the fabricated antenna have verified the effectiveness of the proposed design. Measured results show that the fabricated antenna provides a 53.7% impedance bandwidth ranging from 4.5 to 7.8 GHz and a measured gain better than 4 dBi. Good unidirectional radiation patterns with a high front-to-back ratio greater than 17 dB are achieved.

## 1 Introduction

Owing to their planar structure, broad impedance bandwidth and simple structure, printed double-dipole antennas have been used in many communication applications [1]. The double-dipole antennas usually consist of two dipole elements with different lengths. The long and short dipoles control the lower and upper operating frequencies and then a wideband performance will be obtained when the parameters are properly chosen. Usually, unidirectional radiation patterns with high directivity are urgently required [2]. Therefore several concepts have been adopted to improve the directivity of double-dipole antennas. There are two feeding structures used to feed the double-dipole antenna. One of them is the series-fed structure for double-dipole antenna. Some double-dipole antennas fed by series-fed structures have been proposed and good unidirectional radiation patterns are achieved [3–5]. However, a large size is always needed to obtain high front-to-back (F/B) ratio. Another feeding structure for feeding double-dipole antenna is the parallel-fed structure. When the two dipole elements are fed with a pair of antiphase signals realised by parallel-fed structure, this type of double-dipole antenna is regarded as a W8JK array antenna [6]. Good unidirectional radiation characteristics with high F/B ratio can be achieved [7]. However, it is difficult to realise a pair of antiphase signals to feed this type of antenna in a planar structure. Therefore a new feeding structure is needed to be investigated for feeding this type of double-dipole antenna.

In this study, a planar printed double-dipole antenna with wideband performance and high directivity is proposed.

The wideband performance is achieved by using the two dipole elements with different lengths. High directivity is obtained by feeding the two dipole elements with a pair of antiphase signals. To solve the difficulty of antiphase feeding in a planar structure, a new equivalent feeding mechanism is presented and a new feeding structure based on a microstrip balun and two pairs of parallel striplines is designed. Moreover, an antenna prototype is fabricated and tested to demonstrate the effectiveness of this new feeding mechanism. Good agreement between the simulated and measured results proves the validity of the proposed feeding mechanism for double-dipole antenna. The proposed antenna can achieve a wide impedance bandwidth with a compact size and good unidirectional radiation ability with high F/B ratio. Stable radiation patterns and high F/B ratio can make this antenna to be considered for wideband phased-array antennas, power-combining arrays and multiple-beam arrays.

## 2 Antenna design and feeding structure

### 2.1 Equivalent feeding mechanism

The conventional double-dipole antenna consists of two parallel dipole elements. It can realise bidirectional radiation patterns by feeding the two parallel dipole elements with two opposite phase currents. When the two dipole elements are designed with different lengths and fed by a pair of antiphase signals  $V_1$  and  $V_2$  as shown in Fig. 1a, the phase of the current on the short dipole will be lagging behind that of the current on the long dipole. Then, the short

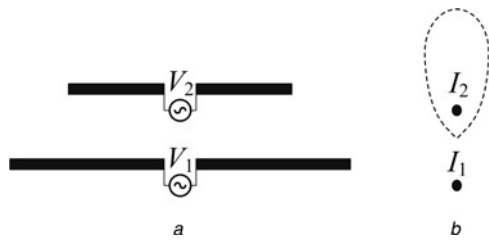


**Fig. 1** Double-dipole antenna with different length elements fed by antiphase signals  
 a Antenna structure  
 b Radiation pattern

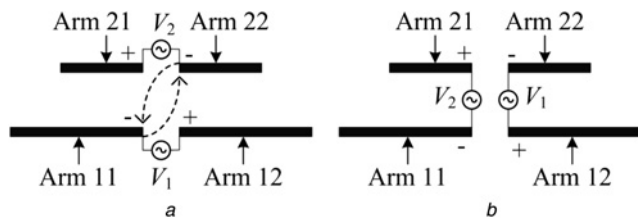


**Fig. 2** Evolution feeding mechanisms of the double-dipole antenna  
 a Initial feeding structure  
 b New equivalent feeding mechanism

dipole element will guide the electromagnetic wave propagation. Therefore the directivity in the short dipole direction is enhanced and the radiation pattern is illustrated in Fig. 1*b*. However, this type of double-dipole antenna requires a pair of antiphase feeding signals. It is difficult to realise a pair of antiphase signals to feed this type of double-dipole antenna in a planar structure. Thus, a new equivalent feeding mechanism is presented in this study to solve this problem.

The evolution of the feeding mechanisms for the double-dipole antenna is shown in Fig. 2. For each dipole element of the double-dipole antenna, one arm is labelled by (+) whereas the other arm is labelled by (-) to indicate the 180° phase difference between them. The initial feeding structure for the double-dipole antenna is shown in Fig. 2*a*. As shown in Fig. 2*a*, the feeding structure is constructed by a pair of antiphase signals  $V_1$  and  $V_2$  with equal magnitude. Owing to the antiphase characteristics of the signals  $V_1$  and  $V_2$ , we can consider the left arms and right arms of the double-dipole antenna as two new equivalent dipoles,

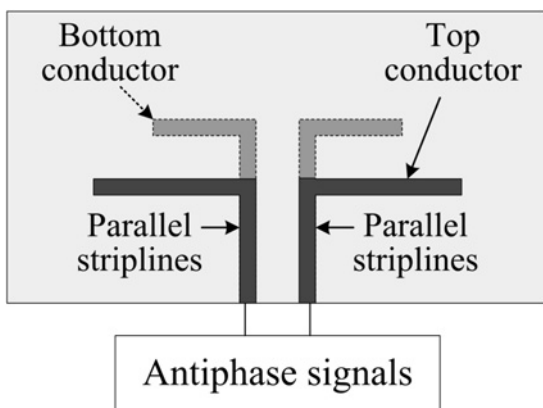


**Fig. 3** Layout of the equivalent feeding mechanism for the double-dipole antenna

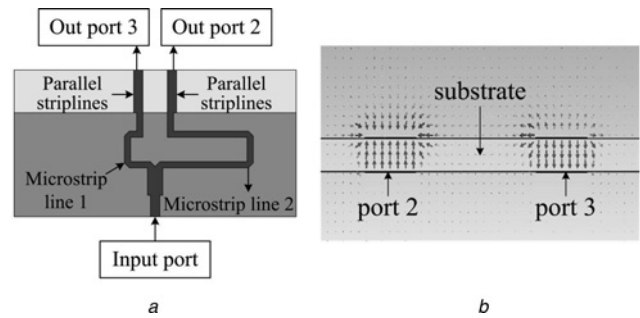


**Fig. 4** Designed feeding structure based on a microstrip balun and parallel striplines  
 a Layout  
 b Simulated electric field distributions of the out ports at 6 GHz

respectively. It means that the double-dipole antenna can be excited in the left and right parts with a pair of antiphase signals. Fig. 2*b* shows the double-dipole antenna with the new equivalent feeding mechanism. Because the two feeding signals  $V_1$  and  $V_2$  are antiphase with equal magnitude, the currents on the arms of the double-dipole antenna are not changed when the equivalent feeding mechanism is adopted. This means that the radiation characteristics of the double-dipole antenna will not be changed by using this new equivalent feeding mechanism. However, it is easier to realise this new feeding mechanism for the double-dipole antenna in a planar structure.

To realise the new feeding mechanism for the double-dipole antenna, two pairs of parallel striplines are used. The layout of the double-dipole antenna with the two pairs of parallel striplines is shown in Fig. 3. As shown in the figure, the short dipole is printed on the bottom layer of the substrate and the long dipole is printed on the top layer of the substrate. The arms of the short dipole are connected to the bottom metal strips of the parallel striplines whereas the arms of long dipole are connected to the top metal strips of the parallel striplines. A pair of antiphase signals is used to excite the parallel striplines. In this study, a new feeding structure based on a microstrip balun previously reported in [8] is designed to realise a pair of antiphase signals to excite the two pairs of parallel striplines.

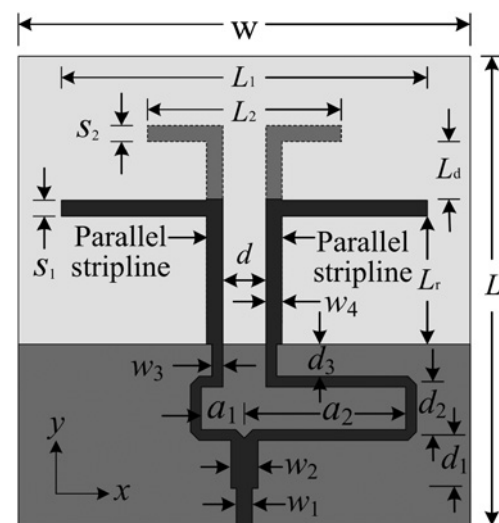


**Fig. 5** Schematic configuration and parameters of the proposed designed antenna

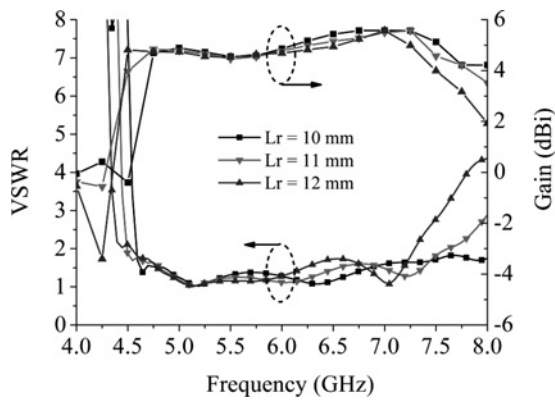


Fig. 6 Effect of the distance ( $L_r$ ) between the long dipole and ground plane

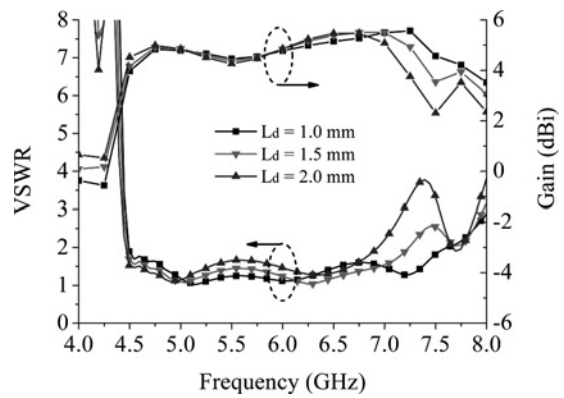


Fig. 8 Effect of the distance ( $L_d$ ) between the two dipole elements

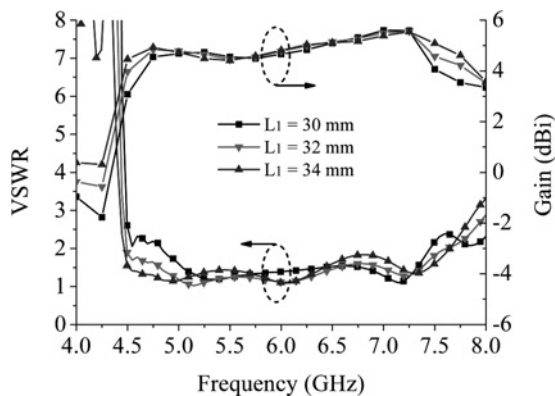


Fig. 7 Effect of the length ( $L_l$ ) of the long dipole

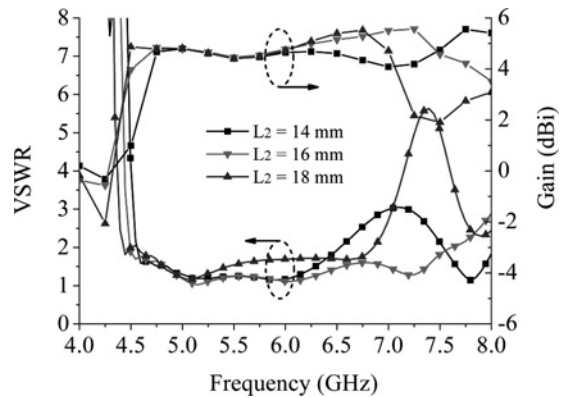


Fig. 9 Effect of the length ( $L_2$ ) of the short dipole

The layout of the designed feeding structure based on a microstrip balun is shown in Fig. 4a. The T-junction is used for signal dividing. To facilitate a signal dividing with antiphase characteristics, microstrip line 2 is prolonged to ensure that it is  $180^\circ$  out of phase compared with microstrip line 1. Fig. 4b illustrates the simulated electric field distributions at 6 GHz at the out ports. It is observed that the electric fields at the out ports are antiphase. Thus this feeding structure can be used to realise a pair of antiphase signals for feeding the double-dipole antenna.

## 2.2 Antenna structure and parametric study

Putting the radiation elements and the feeding structure together, a double-dipole antenna with new feeding structure is obtained. The layout of the designed antenna is illustrated in Fig. 5. This antenna is printed on a piece of FR-4 substrate with a relative permittivity of 4.4 and a thickness of 0.8 mm. The two dipole elements are connected to the out ports of the microstrip balun through two pairs of parallel striplines. In addition, the ground plane serves as a reflector element for the designed antenna.

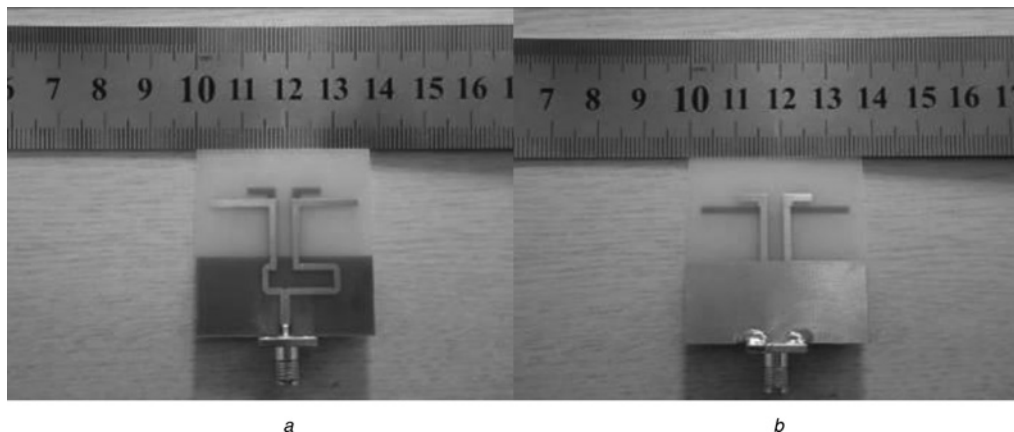
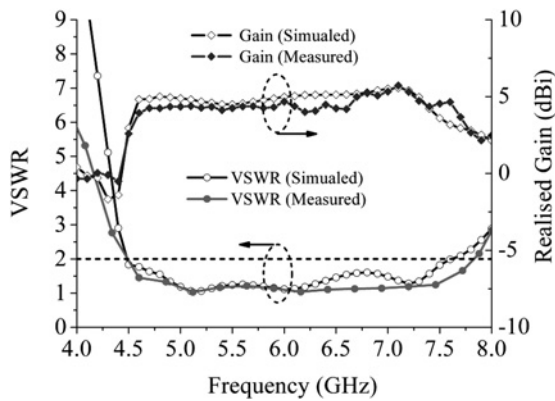


Fig. 10 Photographs of the fabricated antenna

a Top layer  
b Bottom layer



**Fig. 11** Measured and simulated VSWR results and antenna gains of the proposed antenna

Therefore it will further enhance the directivity of the proposed antenna.

To understand the behavior of the designed antenna, a parametric study is performed. Figs. 6 and 7 show the effect of the long dipole parameters on the voltage standing wave ratio (VSWR) result and antenna gain. As shown in Fig. 6, the parameter  $L_r$  decides the bandwidth of the designed antenna. As  $L_r$  is increased, the bandwidth is shifted to low frequencies. For an acceptable impedance bandwidth and antenna gain,  $L_r$  was set to be 11 mm. Fig. 7 shows that the length ( $L_1$ ) of the long dipole is the main parameter that affects the performance of the antenna at the low frequencies.  $L_1$  was set to be 32 mm for good performance. Figs. 8 and 9

show the effect of the short dipole parameters. Fig. 8 shows that the VSWR and antenna gain are sensitive to the distance ( $L_d$ ) at the 7.3 GHz.  $L_d$  was set to be 1 mm for an acceptable performance. Fig. 9 shows that the VSWR and gain are very sensitive to the length ( $L_2$ ) of short dipole at high frequencies. For a wide impedance bandwidth and high gain,  $L_2$  was set to be 16 mm.

From the above discussions, we can conclude that the new feeding structure for feeding the double-dipole antenna is very effective. To achieve a wide impedance bandwidth and high directivity, the dimensions of the designed antenna are optimised. By optimisation, the final dimensions of the proposed antenna are as follows:  $S_1 = 1.6$  mm,  $S_2 = 1.6$  mm,  $W = 38$  mm,  $W_1 = 1.5$  mm,  $W_2 = 2$  mm,  $W_3 = 1.3$  mm,  $W_4 = 1.5$  mm,  $d = 3.5$  mm,  $d_1 = 6.8$  mm,  $d_2 = 5$  mm,  $d_3 = 1.7$  mm,  $a_1 = 3.5$  mm,  $a_2 = 10.5$  mm,  $L = 40$  mm,  $L_r = 11$  mm,  $L_d = 1$  mm,  $L_1 = 32$  mm,  $L_2 = 16$  mm. The overall substrate size of the antenna is  $W \times L = 38$  mm  $\times$  40 mm. Measured results will be discussed in the following section.

### 3 Experimental results

Aiming to demonstrate the effectiveness of the proposed design, a prototype of the designed antenna is fabricated and tested. Photographs of the fabricated antenna are shown in Fig. 10. A 50  $\Omega$  SMA connector is used to feed the antenna for measurement. The impedance bandwidth of the fabricated antenna is obtained by using an Agilent E8363B Programmable Network Analyser and the radiation performance is measured by using an SATIMO measurement system.

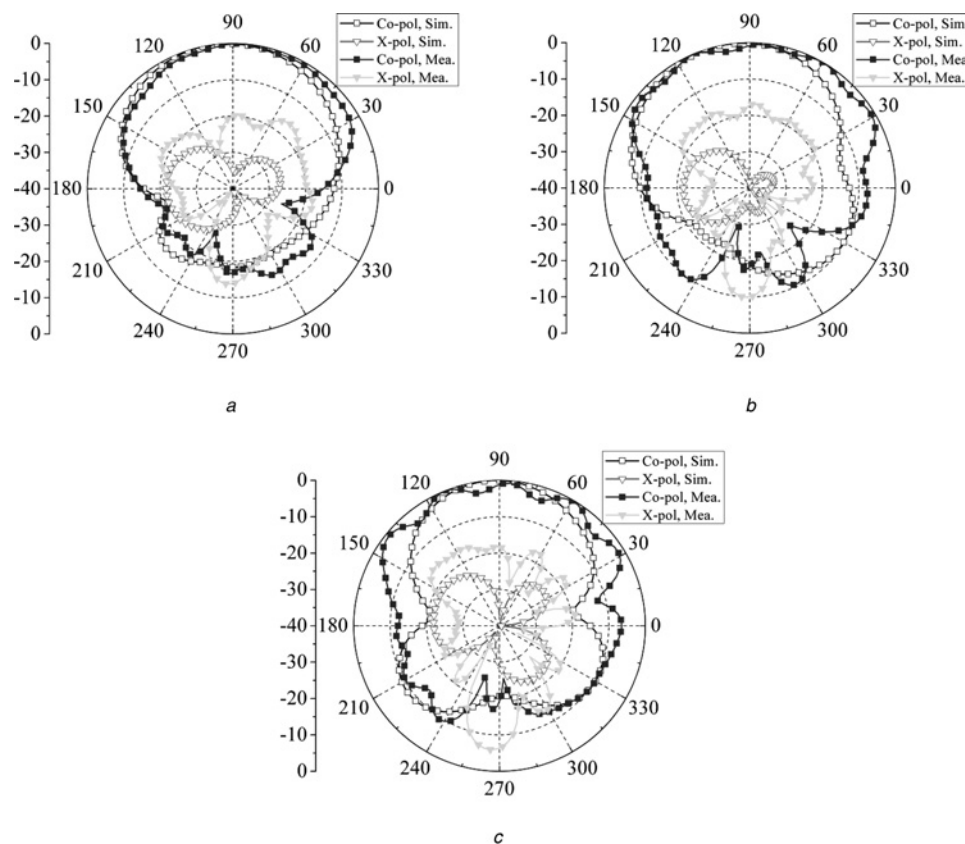


**Fig. 12** Measured and simulated radiation patterns of the proposed antenna in E-plane (xoy-plane) at different frequencies

a 5 GHz

b 6 GHz

c 7 GHz



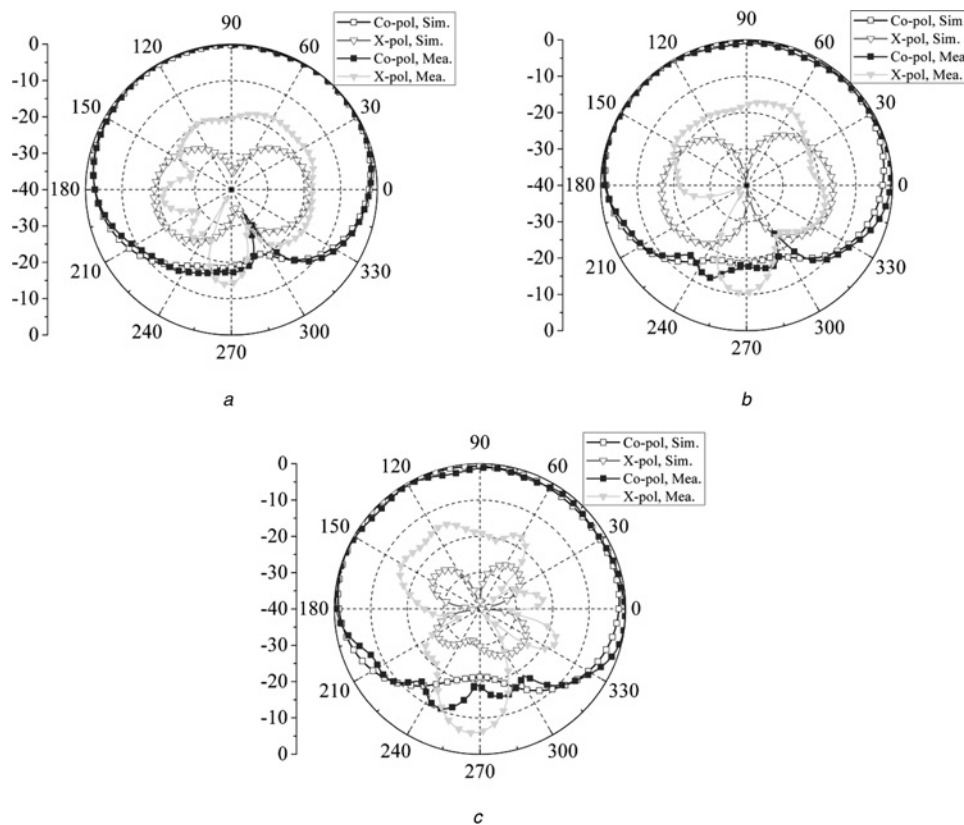


**Fig. 13** Measured and simulated radiation patterns of the proposed antenna in H-plane (*yoz*-plane) at different frequencies

a 5 GHz  
b 6 GHz  
c 7 GHz

The simulated and measured reflection coefficients are shown in Fig. 11. It is observed that the experimental results agree well with the simulation results. As shown in the figure, the simulated impedance bandwidth, defined by  $VSWR < 2$ , is from 4.5 to 7.5 GHz and the measured impedance bandwidth, defined by  $VSWR < 2$ , is from 4.5 to 7.8 GHz, that is, a fractional bandwidth of 53.7%. A wide impedance bandwidth is obtained. The simulated and measured gains of the designed antenna are also plotted in Fig. 11. Good agreement between the measurement and simulation results is also observed. In the band from 4.5 to 7.8 GHz, the minimum gain is at the frequency 6.2 GHz with a value of 4.1 dBi and the maximum gain is at 7.1 GHz with a value of 5.7 dBi. This means that the proposed antenna can realise a wide impedance bandwidth with a moderate gain better than 4 dBi.

In order to illustrate the radiation performance of the designed antenna, its radiation patterns are also measured. The simulated and measured radiation patterns in the *E*-plane (*xoy*-plane) and the *H*-plane (*yoz*-plane) at 5, 6 and 7 GHz are depicted in Figs. 12 and 13, respectively. It is observed from the plots that the measurement results are in good agreement with the simulation results. As shown in the figures, good unidirectional radiation characteristics are both achieved in the *E*-plane and the *H*-plane in the operating frequency band. In addition, the main radiation lobes of the radiation patterns are fixed at the broadside direction. It means that the proposed antenna can provide unidirectional radiation patterns with stable radiation directivity. The measured cross-polarisation characteristics are also depicted in Figs. 12 and 13. According to the measured results, the cross-polarisation levels in the *E*- and

*H*-planes are generally less than  $-17.1$  and  $-15.3$  dB in the broadside direction, respectively. The effectiveness of the designed antenna is further experimentally confirmed according to the measured radiation patterns.

Another critical parameter for a unidirectional antenna is the F/B ratio, which represents the unidirectional radiation capability of the antenna. Therefore the F/B ratio of the designed antenna is also investigated. The simulated and measured F/B ratios of the designed antenna are shown in Fig. 14. As shown in the figure, the measurement results and the simulation results agree well with each other. According to the measured results, the measured F/B ratio is better than 17 dB in the band from 4.5 to 7.5 GHz. Good unidirectional radiation characteristics with a high F/B ratio

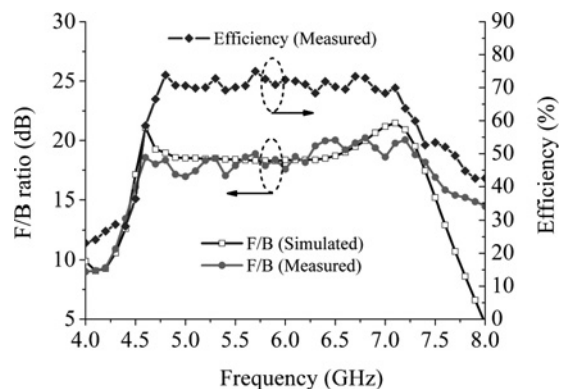


**Fig. 14** Simulated and measured F/B ratio results and the measured radiation efficiency of the proposed antenna

are experimentally confirmed. The measured radiation efficiency of the fabricated antenna is also shown in Fig. 14. The measured radiation efficiency was provided by using the antenna measurement system, SATIMO system. The measured value includes the impacts from mismatch loss, dielectric loss. For most of the operating frequency band (4.6–7.2 GHz), the measured radiation efficiency of the fabricated antenna is around 70%.

As compared with the proposed antenna, the double-dipole antennas in [1, 3] have similar sizes compared with the proposed antenna, but the proposed antenna realises a relatively wide impedance bandwidth with a higher F/B ratio. The double-dipole antenna presented in [5] realised a 103% measured bandwidth with the F/B ratio better than 16 dB. Its size is  $2.78 \lambda_g \times 4.33 \lambda_g$ . Here,  $\lambda_g$  is referred to as the guided wavelength of a conventional  $50 \Omega$  microstrip line at the same frequency. For the proposed double-dipole antenna, the size is about  $1.42 \lambda_g \times 1.49 \lambda_g$  at the centre operating frequency, that is, 6.15 GHz. It means that the proposed antenna can achieve wide impedance and high F/B ratio with a relatively small size.

#### 4 Conclusions

A double-dipole antenna with wideband performance and unidirectional radiation patterns is proposed in this study. The wideband performance is obtained by designing the two dipole elements with different lengths. The unidirectional radiation characteristics are realised by feeding the two dipole elements with a pair of antiphase feeding signals. To solve the difficulty of realising a pair of antiphase signals for feeding the double-dipole antenna in a planar structure, a new equivalent feeding mechanism is presented and a new feeding structure is designed to realise the two antiphase signals for exciting the double-dipole antenna. Experimental results of the fabricated prototype verified the effectiveness of the proposed feeding structure.

According to the measured results, the fabricated antenna exhibits excellent unidirectional radiation patterns with a high F/B ratio better than 17 dB. A moderate gain better than 4 dBi and a fractional bandwidth of 53.7% ranging from 4.5 to 7.8 GHz are also obtained.

#### 5 Acknowledgments

This work was supported in part by the National Natural Science Foundation of China by Grants (61171044 and 61231001), the Fundamental Research Funds for the Central Universities of China (ZYGX2012YB010 and ZYGX2012Z005), and Research Fund for the Doctoral Program of Higher Education of China (20120185110024).

#### 6 References

- 1 Yeo, J., Lee, J.-I.: 'Modified series-fed two-dipole-array antenna with reduced size', *IEEE Antennas Wirel. Propag. Lett.*, 2013, **12**, pp. 214–217
- 2 Thai, T.T., DeJean, G.R., Tentzeris, M.M.: 'Design and development of a novel compact soft-surface structure for the front-to-back ratio improvement and size reduction of a microstrip yagi array antenna', *IEEE Antennas Wirel. Propag. Lett.*, 2008, **7**, pp. 369–373
- 3 Yeo, J., Lee, J.-I.: 'Broadband series-fed two dipole array antenna with an integrated balun for mobile communication applications', *Microw. Opt. Technol. Lett.*, 2012, **54**, (9), pp. 2166–2168
- 4 Eldek, A.A.: 'Design of double dipole antenna with enhanced usable bandwidth for wideband phased array applications', *Prog. Electromagn. Res.*, 2006, **59**, pp. 1–15
- 5 Eldek, A.A.: 'Ultrawideband double rhombus antenna with stable radiation patterns for phased array applications', *IEEE Trans. Antennas Propag.*, 2007, **55**, (1), pp. 84–91
- 6 Kraus, J.D., Marhefka, R.J.: 'Antennas for all applications' (McGraw-Hill, New York, 2002, 3rd edn.)
- 7 Gustafson, E.S.: 'Two-element driven array with improved tuning and matching'. US Patent No. 6, 411, 264, 25 June 2002
- 8 Kaneda, N., Deal, W.R., Qian, Y., Waterhouse, R., Itoh, T.: 'A broad-band planar quasi-yagi antenna', *IEEE Trans. Antennas Propag.*, 2002, **50**, (8), pp. 1158–1160

Copyright of IET Microwaves, Antennas & Propagation is the property of Institution of Engineering & Technology and its content may not be copied or emailed to multiple sites or posted to a listserv without the copyright holder's express written permission. However, users may print, download, or email articles for individual use.